ce/papers Proceedings in civil engineering

Ernst & Sohn A Wiley Brand

ORIGINAL ARTICLE

eurosteel AMSTERDAM 2023

Ernst & Sohn A Wiley Brand

Fatigue strengthening of cracked steel plates with bonded Fe-SMA strips

Lingzhen Li[1,2] | Sizhe Wang[1,3] | Tao Chen[3] | Eleni Chatzi[2] | Hossein Heydarinouri[1] | Elyas Ghafoori[4]

Correspondence

Mr. Lingzhen Li
Empa, Swiss Federal Laboratories for Materials Science and Technology, Structural Engineering Research Laboratory
8600, Dübendorf, Switzerland
Email: lingzhen.li@empa.ch

[1] Empa, 8600, Dübendorf, Switzerland
[2] ETH Zürich, 8093, Zürich, Switzerland
[3] Tongji University, 200092, Shanghai, China
[4] Leibniz University Hannover, 30167, Hannover, Germany

Abstract

Prestressed fatigue strengthening of steel structures has been proven effective by numerous investigations. Bonded iron-based shape memory alloy (Fe-SMA) strengthening has shown a great potential in this regard, however, with limited corroborating studies. Moreover, a proper model for fatigue analysis of systems that are retrofitted with bonded Fe-SMA strengthening is missing. In this study, an analytical model, coupling prestress analysis and fatigue analysis, is proposed. Four steel plates with central through-thickness cracks were strengthened with use of bonded Fe-SMA strips, and subsequently tested under fatigue loading after generating prestress via heating and cooling. The fatigue behavior predicted by the proposed model lies in excellent agreement with the fatigue testing results.

Keywords

Fe-SMA, bonded strengthening, prestress loss, fatigue crack arrest

1 Introduction

Prestressed strengthening against fatigue crack initiation and propagation in steel structures has been proven effective in recent literature [1, 2]. Bonded iron-based shape memory alloys (Fe-SMAs) offer a promising solution in this regard. Wang et al. [3] proposed a strengthening solution with partial activation, as illustrated in Figure 1 and Figure 2. The prestrained Fe-SMA strips are bonded onto the target structure, with their middle segments (activation zone) heated to generate prestress, while the remaining two ends (bonded anchorage zones) remain unheated and transfer the prestress to the parent structure. Fatigue lives of cracked steel plates strengthened by this solution were enhanced substantially compared with the unstrengthened one [3].

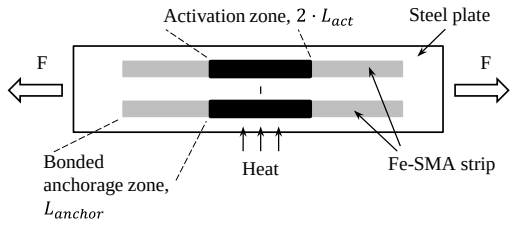

Figure 1 Top view of a steel plate with a central crack strengthened with Fe-SMA strips.

As this is an emerging solution, the related investigations remain limited, while a proper model for predicting the fatigue behavior of steel structures after the bonded Fe-SMA strengthening is missing.

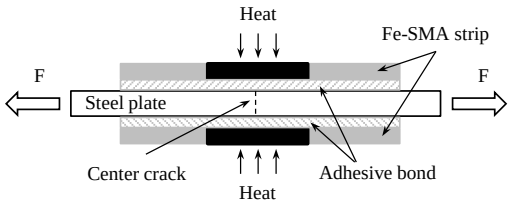

Figure 2 Side view of a steel plate with a central crack strengthened with Fe-SMA strips.

In this study, a model, coupling a prestress and fatigue analysis, is proposed. Four steel plates with central through thickness cracks are strengthened by bonded Fe-SMA strips and tested under fatigue loading, with the results used for validation of the proposed model.

2 Strengthening analysis

2.1 Prestress analysis

To enhance the fatigue performance of steel plates with central through-thickness cracks, Fe-SMA strips are

https://doi.org/10.1002/cepa.2559

bonded on both sides of steel plates. The activation zone of each Fe-SMA strip is heated to a certain temperature to generate prestress, while the bonded anchorage zones, which remain unheated, transfer the generated prestress to substrate steel plates. Figure 3 illustrates the free body diagram of a strengthened plate. The activation zone of the Fe-SMA strip, comprising a length of L_{act} =200 mm, is heated to a target temperature of 120, 180, or 260 °C to generate prestress, during which the adhesive loses most of its stiffness. This allows for assuming the adhesive layer within the activation zone as fully soft during activation. Li et al. [4] reported that, when the activation zone cools to the room temperature, it features a considerable shear capacity, which implies that the adhesive re-cures after activation. If the Fe-SMA strips are split at the center line, they shrink during the activation, as demonstrated in Figure 3 (b), which reflects the shape memory effect. However, the Fe-SMA strips and steel plate deform simultaneously, as illustrated in Figure 3 (c). The analysis of the prestress level, which is proposed by the authoring team [5], is briefly explained in what follows.

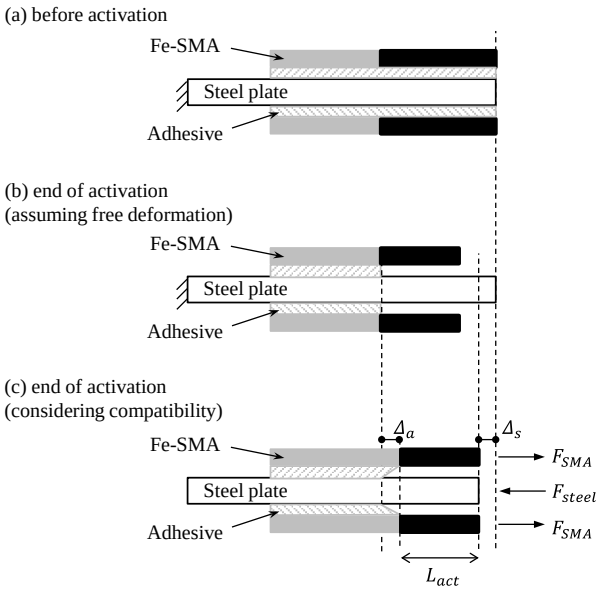

Figure 3 Schematic view of a strengthened steel plate with bonded Fe-SMA, only half of the system is shown, due to symmetry [5].

The equilibrium of Figure 3 (c) is expressed in terms of Equations (1-3). The Fe-SMA strip lies in equilibrium under tension generated in the activation zone and shear in the bonded anchorage zone, as represented by Equation (4).

$$2 \cdot F_{SMA} = F_{steel} \tag{1}$$

$$F_{SMA} = \sigma_{pre} \cdot A_{SMA} \tag{2}$$

$$F_{steel} = \sigma_{steel} \cdot A_{steel} \tag{3}$$

$$F_{SMA} = f_{F-\Delta}(\Delta_a) \tag{4}$$

where F_{SMA} and A_{SMA} represent the tensile force and cross-sectional area of Fe-SMA strips on one side of the steel plate; F_{steel} and A_{steel} denote the compressive force and cross-sectional area of the steel plate. σ_{pre} is the prestress generated in the Fe-SMA strip, while σ_{steel} is the compressive stress in the steel plate; $f_{F-\Delta}$ represents the load-displacement behavior of the adhesive joint, whose shear deformation is represented as Δ_a.

To measure the prestress at different activation temperatures, Fe-SMA samples are usually held by a testing machine of large stiffness, with the measured stress referred to as the recovery stress (σ_{rec}). In the case of prestressed strengthening, the finally applied prestress (σ_{pre}) experiences a lower value, due to the prestress loss (σ_{loss}), resulting from the finite stiffness of the substrate structure etc. The prestress can be computed by Equation (5). In this study, two sources of prestress loss are considered, namely the compression of the steel plate (Δ_s) and the shear deformation of the adhesively bonded joint (Δ_a), as illustrated in Figure 3 (c) and expressed as Equation (6). The compressive stress held in the steel plate is expressed as Equation (7).

$$\sigma_{pre} = \sigma_{rec} - \sigma_{loss} \tag{5}$$

$$\sigma_{loss} = \frac{\Delta_s + \Delta_a}{L_{act}} \cdot E_{SMA} \tag{6}$$

$$\sigma_{steel} = \frac{\Delta_s}{L_{act}} \cdot E_{steel} \tag{7}$$

where σ_{rec} and σ_{pre} are the recovery stress and prestress, respectively; σ_{loss} means the prestress loss; L_{act} represents half of the activation length; E_{SMA} is the secant modulus of the Fe-SMA at the quasi-linear stage; E_{steel} denotes the E-modulus of the steel plate.

By substituting Equations (2, 3, 5, 6, and 7) into Equation (1), one can derive Equation (8). Additionally, one can express Equation (4) in a new form as Equation (9).

$$\Delta_s = \frac{2 \cdot \sigma_{rec} \cdot L_{act} \cdot A_{SMA} - 2 \cdot \Delta_a \cdot E_{SMA} \cdot A_{SMA}}{E_{steel} \cdot A_{steel} + 2 \cdot E_{SMA} \cdot A_{SMA}} \tag{8}$$

$$\left(\sigma_{rec} - \frac{\Delta_s + \Delta_a}{L_{act}} \cdot E_{SMA}\right) \cdot A_{SMA} = f_{F-\Delta}(\Delta_a) \tag{9}$$

The solution of Equations (8 and 9) via an iterative numerical scheme yields the states at the end of activation, such as the prestress loss, the level of retained prestress in the strengthening system, and the deformations of both the steel plate and the adhesive joint.

A transition zone, between the activation zone and bonded anchorage zone, should exist to accommodate the temperature gradient from the activation temperature to the room temperature. In this transition zone, a certain level of prestress is generated, while the underneath adhesive is softened to some extent. The transition zone is ignored in the current model analysis, resulting in some level of error. Nevertheless, a study [5] targeting at a thorough prestress analysis demonstrates that, despite the transition zone, the simplified model still yields a satisfactory prestress prediction, in terms of applied compression in the steel substrate.

2.2 Fatigue analysis

After applying the prestress via heating and subsequent cooling, the specimen illustrated in Figure 1 (a) is tested under cyclic loading with a constant stress range ($\Delta\sigma =$

$\sigma_{max} - \sigma_{min}$) with a stress ratio ($R = \sigma_{min}/\sigma_{max}$) of 0.1. This section provides an analytical solution for the determination of whether a fatigue crack propagates.

In this study, steel plates are 850 mm long, 150 mm wide, and 10 mm thick, with a central through-thickness crack whose length is 15 mm ($2a = 15$ mm, with a being the half crack length). Four Fe-SMA strips, each with a dimension of $500 \times 50 \times 1.5$ (length × width × thickness, in mm), are bonded on both sides of a steel plate, without covering the crack. According to a previous study [6] with a numerical analysis, the external load is transferred from the steel plate to the strengthening strips via the shear stress at the bonded anchorage zone. Since the Fe-SMA strips do not cover the crack, no or negligible shear stress is developed in the activation zone. This allows for a load distribution among the steel plate and Fe-SMA strips via the stiffness ratio (ρ) of cross-sections, expressed as Equation (13), facilitating the fatigue analysis.

The stress intensity factor (SIF, denoted as K) describes the stress field in the vicinity of the crack tip. Figure 4 demonstrates a plate with a finite width and a central crack, in which the SIF can be estimated via Equations (10-11) [7]. Considering the extra stiffness that bonded Fe-SMA strips contribute and the applied prestressing force, the far-field stress (σ_{far}) with respect to the cracked section after strengthening should be corrected by Equations (12-13). In the strengthening scheme, each side of the cracked steel plate is bonded with two Fe-SMA strips with a total width of 100 mm, as schematically illustrated in Figure 1. The distance between two Fe-SMA strips on one side is 30 mm. This allows for a relatively even compression on the cross-section of steel plate. Since the activation length is 200 mm, which means the generated compressive force is applied 100 mm away from the cracked section. This further smoothens the distribution of compressive stress in the cracked section. As a result, the prestressing effect is considered as an evenly distributed compression at the cracked section in the current model.

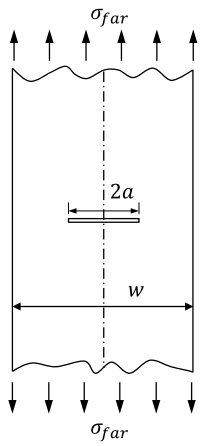

Figure 4 Crack analysis.

$$K = F_{corr} \cdot \sigma_{far} \cdot \sqrt{\pi \cdot a} \tag{10}$$

$$F_{corr} = \frac{1 - 0.5\left(\frac{2a}{w}\right) + 0.326\left(\frac{2a}{w}\right)^2}{\sqrt{1 - \frac{2a}{w}}} \tag{11}$$

$$\sigma_{far} = \rho \cdot \sigma_0 - \sigma_{pre} \cdot \frac{2 \cdot A_{SMA}}{A_{steel}} \tag{12}$$

$$\rho = \frac{E_{steel} \cdot A_{steel}}{E_{steel} \cdot A_{steel} + 2 \cdot E_{SMA} \cdot A_{SMA}} \tag{13}$$

where F_{corr} is a geometric correction factor considering the finite plate width; a and w represent the half crack length and plate width; σ_0 denotes the tensile stress in the cross-section without strengthening; σ_{pre} is computed from a previous section.

In the fatigue analysis, the SIF range, rather than the absolute SIF value, is of importance. Due to the cyclic plastic deformation at the crack tip, the driving force to open the crack is less than the computation using Equations (10-13). This phenomenon is known as the crack closure effect, to consider which Hosseini et al. [2] figured out a reduction of the SIF range, which is referred to as the effective SIF range (ΔK_{eff}) and expressed as Equation (14). Should be noted that, when the crack tip is under compression, a negative SIF value does not have a physical connotation. Therefore, K_{min} is taken as zero when the crack tip is under compression at the minimum load in a loading cycle. A threshold of the effective SIF range exists, below which no fatigue crack propagates and above which the existing crack propagates [8]. Hosseini et al. [2] reported a range of this threshold as 200-285 MPa·mm$^{1/2}$, which was determined via fatigue tests with different load levels on central cracked steel plates produced by the same manufacturer as those in the current study. Therefore, three zones are defined here with fatigue crack arrest, fatigue crack propagation, and potential crack propagation, as listed in Table 1.

$$\Delta K_{eff} = U \cdot (K_{max} - K_{min}) \tag{14}$$

where $U = 0.9$ considers the crack closure effect [2], with respect to a stress ratio of 0.1; K_{max} and K_{min} represent the maximum and minimum SIF; K_{min} is zero when the crack tip is under compression at the lowest load during a loading cycle.

Table 1 The proposed criterion for determining the onset of crack propagation

Effective SIF range (MPa·mm$^{1/2}$)	Consequence
$\Delta K_{eff} \leq 200$	Crack arrest
$200 < \Delta K_{eff} < 285$	With chance of propagation
$\Delta K_{eff} \geq 285$	Crack propagation

Three specimens (SP-Act120, SP-Act180, and SP-Act260) with different prestress levels are analysed. Their activation zones are heated to 120, 180, and 260 °C, respectively, with generated recovery stress (σ_{rec}) values of 230, 320, and 400 MPa, respectively [9-12]. In each specimen, three or four load levels are applied, which are $\Delta\sigma$ = 60, 75, 90, and 105 MPa. Substituting the geometry, applied load, and generated recovery stress into Equations (5-6, 8-14), the effective SIF range (ΔK_{eff}) at the crack tip is

computed. Further substituting the estimated ΔK_{eff} into Table 1, one determines whether the existing crack after strengthening propagates. Figure 5 summarizes the prediction of three specimens under different fatigue load levels. It suggests that specimens SP-Act120 and SP-Act260 at the load levels of $\Delta\sigma = 90$ MPa and $\Delta\sigma = 105$ MPa, respectively, have fatigue crack propagation, while specimen SP-Act180 at the load level of $\Delta\sigma = 90$ MPa has a high chance of propagation. SP-Act120 and SP-Act260 at the load levels of $\Delta\sigma = 75$ MPa and $\Delta\sigma = 90$ MPa, respectively, have a low chance of crack propagation. The rest are expected to survive without any crack propagation.

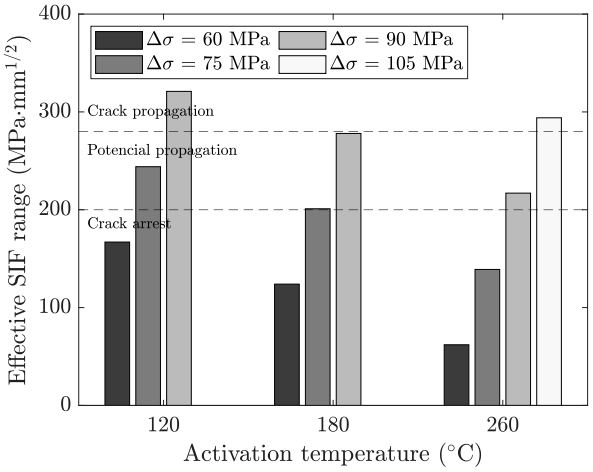

Figure 5 Prediction of fatigue crack propagation.

3 Experimental validation

3.1 Fatigue test

Four steel plates with central through-thickness cracks were strengthened by bonded Fe-SMA strips. The central cracks, with a length of 15 mm and blunt crack tips, were cut with electrical discharging. Prior to bonding Fe-SMA strips, bare plates were fatigued with constant stress range ($\Delta\sigma = 75$ MPa) , until a precrack length of ca. 1 mm, allowing for a natural sharp crack tip. Details of precracking are provided in Table 2.

Table 2 Pre-cracking details

Specimen symbol	$\Delta\sigma$ (MPa)	Precracing cycles	Crack length after pre-cracking, $2a$ (mm)
SP-Act120	75	200,000	17.592
SP-Act180	75	250,000	19.068
SP-Act260-1	75	360,000	18.676
SP-Act260-2	75	220,000	19.896

After the precracking, the bonding areas of steel plates and Fe-SMA strips were cleaned with acetone and sand-blasted to remove the oxidized layer and enhance the surface roughness. Fe-SMA strips were then bonded onto steel plates with an epoxy adhesive, SikaPower 1277, and cured for two weeks. The prestress was generated via electrical resistance heating, after which fatigue tests were conducted. These four fatigue specimens, as listed in Table 3, correspond to the three analysed in the previous section; SP-Act260-1 and SP-Act260-2 are repetition of each other.

Every specimen was loaded starting from a low load level ($\Delta\sigma = 75$ MPa) for 2 million cycles, after which the crack tip was examined by a travelling microscope. If the crack propagation is less than 0.2 mm after 2 million cycles, corresponding to the criterion of 10^{-10}m/cycle [13], it is regarded as a fatigue crack arrest, and 2 more million cycles were applied at an increased load level by adding 15 MPa. A stress ratio of 0.1 was applied for all fatigue loads. All four specimens were tested until they failed at a certain load level, as illustrated in Figure 6.

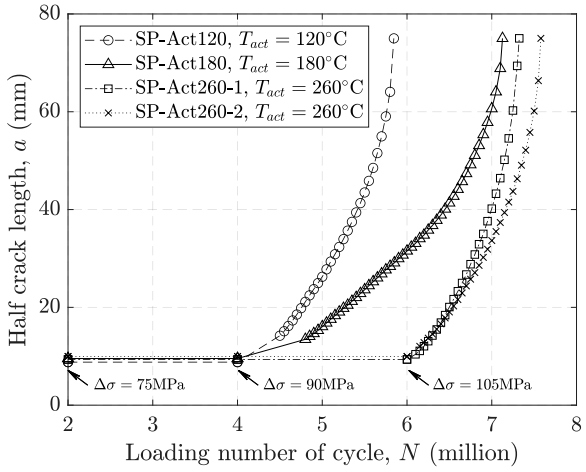

Figure 6 Fatigue testing results.

3.2 Comparison with model prediction

Table 3 lists the fatigue testing results, in comparison with the model predictions. Those at load levels with a prediction of crack arrest ("Arrest" in Table 3) survived after 2 million cycles without crack propagation, while those at load levels with a prediction of crack propagation ("Prop" in Table 3) underwent failure due to growing cracks. Among the four, which were predicted with a chance of crack propagation ("Oppo" in Table 3), the one with a high chance of propagation (SP-Act180 at $\Delta\sigma = 90$ MPa) experienced crack propagation with a finite fatigue life. The other three with a low chance of propagation resisted 2 million cycles fatigue load without an observed propagation. This means the proposed fatigue analysis model, in combination with the prestress analysis model, is capable of accurately determining whether the fatigue crack propagates at a given load level. The fatigue behaviour after the onset of crack propagation is not analysed, since it is outside the scope of the current study.

4 Conclusions

We propose an analytical model, comprising a prestress and fatigue crack analysis, for modelling the behaviour of cracked steel plates that are strengthened with bonded Fe-SMA strips. Four steel plates with central through-thickness cracks were strengthened by bonded Fe-SMA, with prestress generated via electrical resistance heating. Fatigue tests were conducted on the strengthened plates. The proposed model can accurately predict whether fatigue cracks after strengthening propagate. This successful application of prestressed strengthening employing bonded Fe-SMA in the laboratory offers an important step toward its engineering application.

Table 3 Test matrix.

Specimen symbol	Activation temperature (°C)	$\Delta\sigma$ = 75 MPa		$\Delta\sigma$ = 90 MPa		$\Delta\sigma$ = 105 MPa	
		Model prediction	Test result	Model prediction	Test result	Model prediction	Test result
SP-Act120	120	Oppo[a] (244)	Arrest	Prop[b] (321)	Prop[b]	N/A	N/A
SP-Act180	180	Arrest (201)	Arrest	Oppo[a] (278)	Prop[b]	N/A	N/A
SP-Act260-1	260	Arrest (139)	Arrest	Oppo[a] (217)	Arrest	Prop[b] (294)	Prop[b]
SP-Act260-2	260	Arrest (139)	Arrest	Oppo[a] (217)	Arrest	Prop[b] (294)	Prop[b]

[a]with opportunity of crack propagation
[b]crack propagation
Values appearing in brackets are the effective SIF values, in MPa·mm$^{1/2}$

References

[1] Ghafoori, E.; Motavalli, M.; Nussbaumer, A.; Herwig, A.; Prinz, GS.; Fontana, M. (2017) *Design criterion for fatigue strengthening of riveted beams in a 120-year-old railway metallic bridge using pre-stressed CFRP plates*. Composites Part B: Engineering. 68, pp: 1-13.

[2] Hosseini, A.; Ghafoori, E.; Motavalli, M.; Nussbaumer, A.; Zhao, X-L. (2017) *Mode I fatigue crack arrest in tensile steel members using prestressed CFRP plates*. Composite Structures. 178, pp: 119-34.

[3] Wang, W.; Li, L.; Hosseini, A.; Ghafoori, E. (2021) *Novel fatigue strengthening solution for metallic structures using adhesively bonded Fe-SMA strips: A proof of concept study*. International Journal of Fatigue. 148, pp: 106237.

[4] Li, L.; Chatzi, E.; Czaderski, C.; Ghafoori, E. (2023) *Influence of the activation temperature and prestress on the behavior of Fe-SMA-to-steel bonded joints*. Submitted to Construction and Building Materials.

[5] Li, L.; Wang, S.; Chatzi, E.; Motavalli, M.; Ghafoori, E. (2023) *Prediction of prestress level in steel structures strengthened by bonded Fe-SMA strips*. 10th Eurosteel. Amsterdam2023.

[6] Li, L.; Chen, T.; Liu, R. (2021) Rapid SIF Calculation of *Inclined Cracked Steel Plates Bonded with CFRP Materials, Prestressed and Non-prestressed*. 10th International Conference on FRP Composites in Civil Engineering. Springer. pp: 2247-57.

[7] Tada, H.; Paris, P.; Irwin, G. (2000) *The Stress Analysis of Cracks Handbook*. New York, USA. ASME Press.

[8] Institution BS. (2005) *Guide on methods for assessing the acceptability of flaws in metallic structures*. London, UK. British Standard Institution.

[9] Shahverdi, M.; Michels, J.; Czaderski, C.; Motavalli, M. (2018) *Iron-based shape memory alloy strips for strengthening RC members: Material behavior and characterization*. Construction and Building Materials. 173, pp: 586-99.

[10] Izadi, MR.; Ghafoori, E.; Motavalli, M.; Maalek, S. (2018) *Iron-based shape memory alloy for the fatigue strengthening of cracked steel plates: Effects of re-activations and loading frequencies*. Engineering Structures. 176, pp: 953-67.

[11] Izadi, MR.; Ghafoori, E.; Shahverdi, M.; Motavalli, M.; Maalek, S. (2018) *Development of an iron-based shape memory alloy (Fe-SMA) strengthening system for steel plates*. Engineering Structures. 174, pp: 433-46.

[12] Gu, XL.; Chen, ZY.; Yu, QQ.; Ghafoori, E. (2021) *Stress recovery behavior of an Fe-Mn-Si shape memory alloy*. Engineering Structures. 243, pp: 112710.

[13] ASTM. (2002) *Standard test method for measurement of fatigue crack growth rates*. USA. ASTM Press.